5 June 1997

Measurement of the $\omega \to \eta\gamma$ decay branching ratio

Crystal Barrel Collaboration

A. Abele[h], J. Adomeit[g], C. Amsler[p], C.A. Baker[e], B.M. Barnett[c], C.J. Batty[e], M. Benayoun[n], A. Berdoz[m], K. Beuchert[b], S. Bischoff[h], P. Blüm[h], K. Braune[l], J. Brose[k1], D.V. Bugg[i], T. Case[a], A.R. Cooper[i], O. Cramer[l], K.M. Crowe[a], T. Degener[b], H.P. Dietz[l], N. Djaoshvili[f], S. v. Dombrowski[p2], M. Doser[f], W. Dünnweber[l], D. Engelhardt[h], M.A. Faessler[l], P. Giarritta[p], R. Hackmann[c], R.P. Haddock[j], F.H. Heinsius[a], M. Heinzelmann[p], M. Herz[c], N.P. Hessey[l], P. Hidas[d], C. Hodd[i], C. Holzhaußen[h], D. Jamnik[l3], H. Kalinowsky[c], B. Kalteyer[c], B. Kämmle[g], P. Kammel[a], T. Kiel[h], J. Kisiel[f4], E. Klempt[c], H. Koch[b], C. Kolo[l], M. Kunze[b], M. Lakata[a], R. Landua[f], J. Lüdemann[b], H. Matthäy[b], R. McCrady[m], J. Meier[g], C.A. Meyer[m], L. Montanet[f], A. Noble[p5], R. Ouared[f], F. Ould-Saada[p], K. Peters[b], C. Pietra[p6], C.N. Pinder[e], G. Pinter[d], C. Regenfus[l], J. Reißmann[g], S. Resag[c], W. Röthel[l], E. Schäfer[k7], P. Schmidt[g], I. Scott[i], R. Seibert[g], S. Spanier[p], H. Stöck[b], C. Straßburger[c], U. Strohbusch[g], M. Suffert[o], U. Thoma[c], M. Tischhäuser[h], D. Urner[p8], C. Völcker[l], F. Walter[k], D. Walther[b], U. Wiedner[g], B.S. Zou[i] and Č. Zupančič[l].

To be submitted to Phys. Lett. B

[a] University of California, LBL, Berkeley, CA 94720, USA
[b] Universität Bochum, D-44780 Bochum, FRG
[c] Institut für Strahlen- und Kernphysik der Universität Bonn, D-53115 Bonn, FRG
[d] Academy of Science, H-1525 Budapest, Hungary
[e] Rutherford Appleton Laboratory, Chilton, Didcot OX11 0QX, UK
[f] CERN, CH-1211 Genève, Switzerland
[g] Universität Hamburg, D-22761 Hamburg, FRG

[1] Now at Universität Dresden, Dresden, Germany
[2] Now at Cornell University, Ithaca, USA
[3] University of Ljubljana, Ljubljana, Slovenia
[4] University of Silesia, Katowice, Poland
[5] Now at CRPP, Ottawa, Canada
[6] This analysis is the diploma work of C. Pietra
[7] Now at Max Planck Institute, München, Germany
[8] Now at the University of Illinois, Urbana, USA

[h] Universität Karlsruhe, D-76021 Karlsruhe, FRG
[i] Queen Mary and Westfield College, London E1 4NS, UK
[j] University of California, Los Angeles, CA 90024, USA
[k] Universität Mainz, D-55099 Mainz, FRG
[l] Universität München, D-80333 München, FRG
[m] Carnegie Mellon University, Pittsburgh, PA 15213, USA
[n] Université Paris VI et VII, F-75251 Paris, France
[o] Centre de Recherches Nucléaires, F-67037 Strasbourg, France
[p] Universität Zürich, CH-8057 Zürich, Switzerland

Abstract

We have measured the branching ratio for the radiative decay $\omega \to \eta\gamma$ with ω mesons produced in antiproton-proton annihilation at rest into $\pi^0\omega$ and $\eta\omega$. Taking into account $\rho - \omega$ mixing we find a branching ratio $B(\omega \to \eta\gamma) = (6.6 \pm 1.7) \times 10^{-4}$, in accord with the constructive interference solution in other experiments. The upper-limit for the direct radiative decay $\omega \to 3\gamma$ is 1.9×10^{-4} at 95% confidence level.

1 Introduction

Radiative meson decays are a testing ground for the naive quark model since their rates can be predicted from SU(3) and the OZI rule [1, 2]. The theoretical prediction for the partial width of the magnetic transition $\omega \to \pi^0\gamma$ was one of the early triumphs of the quark model. However, radiative meson decays are sensitive to SU(3) breaking by electromagnetism and quark masses [3]. In particular, the production and decay of the ω and ρ mesons are coupled by the isospin breaking ω to ρ transition since their masses overlap. The effect of $\rho - \omega$ mixing is essential in processes where ρ production is comparable to or larger than ω production, for example in e^+e^- annihilation where ω and ρ are produced with a relative rate of 1 to 9. The determination of the decay width for $\omega \to \eta\gamma$ varies by a factor of five depending on whether the interference between $\omega \to \eta\gamma$ and $\rho^0 \to \eta\gamma$ is constructive or destructive [4]. A similar effect is observed in photoproduction [5].

Recently, the GAMS Collaboration has determined the $\omega \to \eta\gamma$ decay branching ratio, $(8.3 \pm 2.1) \times 10^{-4}$, using the reaction $\pi^- p \to \omega n$ at large momentum transfers, thus suppressing ρ production [6]. In this paper we report on an alternative measurement of the $\omega \to \eta\gamma$ branching ratio using $\overline{p}p$ annihilation at rest into $\pi^0\omega$ and $\eta\omega$. Due to $\rho - \omega$ mixing one expects the measured rates for $\omega \to \eta\gamma$ to be different in these two production channels since the ratio of production branching ratios $\eta\omega/\eta\rho^0$ and $\pi^0\omega/\pi^0\rho^0$ are very different [7, 8]. A combined analysis of $\pi^0\omega$ and $\eta\omega$ including $\rho - \omega$ interference then allows a measurement of the $\omega \to \eta\gamma$ branching ratio and a determination of the relative phase between the ω and ρ amplitudes.

2 Apparatus

The experiment was performed with the Crystal Barrel detector on the C2 beam line at LEAR with 200 MeV/c antiprotons stopping in liquid hydrogen. The target is surrounded by two proportional wire chambers which provide a measurement of charged particles close to the annihilation vertex and serve as a fast charged multiplicity trigger. The inner chamber covers 99%, the outer chamber 97% of 4π solid angle. The proportional chambers are surrounded by a jet drift chamber which measures the $r\phi$ coordinates of charged particles as well as their z coordinates along the beam direction through charge division. The electromagnetic calorimeter is made of 1380 CsI(Tl) crystals with photodiode readout to measure the energy deposit and the angles of photons. The calorimeter covers polar angles θ between 12° and 168° with full coverage in azimuthal angle ϕ. The γ energy resolution is

$$\frac{\sigma(E_\gamma)}{E_\gamma} = \frac{2.5\%}{\sqrt[4]{E\ [\mathrm{GeV}]}}. \tag{1}$$

The spatial resolution is energy-dependent, typically 25 mrad in θ and ϕ. All subdetectors are located in a solenoidal coil providing a homogeneous magnetic field of 1.5 T along the beam axis. A detailed description of the apparatus can be found in ref. [9].

In this work the π^0 and η were detected in their 2γ decay mode. Thus the channels $\pi^0\omega$ and $\eta\omega$ were reconstructed from 0-prong events with five detected γ's. The data were collected by vetoing charged particles in the proportional chambers, thus retaining only all-neutral events which occur with a probability of (3.9 ± 0.3) % in $\overline{p}p$ annihilation at rest [10]. The data set

consists of 15.5 million 0-prong events, corresponding to 396 million annihilations. We now describe the reconstruction of the channels $\eta\omega$ and $\pi^0\omega$ where ω decays to three γ's (for more details see ref. [11]).

3 Data selection

A photon induced shower in the CsI barrel is not restricted to a single crystal but spreads over several neighbouring crystals. Such a cluster of hits can involve up to 20 crystals. The reconstruction algorithm works in several steps. Clusters of adjacent crystals with energy deposits above 1 MeV are first reconstructed. For the present analysis the required minimum cluster energy is 10 MeV. Since showers sometimes overlap, local maxima are then searched within the clusters and the cluster energy is shared among the local maxima. A particle energy deposit (PED) is determined by a group of crystals for which the local maximum has at least 10 MeV energy deposit. However, a spurious PED due to shower fluctuation may appear as a small satellite in the vicinity of the main shower. These so called split-off PEDs can be suppressed in the next step by requiring a minimum ratio of energy deposits for nearby PEDs. The optimum tuning of the minimum PED energy and of the split-off suppressing algorithm depends on the background channels for the annihilation channel under study and is performed by Monte-Carlo simulation using GEANT3 [12].

We then select five PED events and obtain a sample of 1.17 million events. Figure 1 shows the 3γ invariant mass distribution for a subset of the data when assuming total energy and total momentum conservation in $\overline{p}p \to 5\gamma$, e.g. when requiring the total energy to lie beween 1.8 and 2.0 GeV and the total momentum to be less than 0.08 GeV/c. The signal for $\omega \to 3\gamma$ is clearly visible. We now submit the events to a 6C kinematic fit assuming total energy and total momentum conservation, at least one $\pi^0 \to 2\gamma$ (or one $\eta \to 2\gamma$) and $\omega \to 3\gamma$[9]. The combination of γ's assigned to the ω and the η or π^0 which yields the best confidence level is selected. To separate the $\pi^0\omega$ from the $\eta\omega$ data sets we require a confidence level of at least 10% for $\pi^0\omega$ and at most 1% for $\eta\omega$ or, vice-versa, at least 10% for $\eta\omega$ and at most 1% for $\pi^0\omega$. We then obtain 62,853 $\pi^0\omega$ and 54,865 $\eta\omega$ events.

We define the usual Dalitz plot variables

$$x = \frac{T_2 - T_1}{\sqrt{3}Q}, \; y = \frac{T_3}{Q} - \frac{1}{3}, \tag{2}$$

where T_1, T_2, T_3 are the kinetic energies of the γ's in the ω rest frame and $Q = T_1 + T_2 + T_3$. Every event is entered six times to obtain a symmetric representation. The $\omega \to 3\gamma$ Dalitz plots for $\pi^0\omega$ and $\eta\omega$ are shown in fig. 2 and 3, respectively. The prominent bands along the boundaries are due to $\omega \to \pi^0\gamma$ and the weaker bands around the center to $\omega \to \eta\gamma$.

4 Background Contributions

The main background contributions to the Dalitz plots (fig. 2 and 3) stem from 6γ events ($\overline{p}p \to 3\pi^0, 2\pi^0\eta, 2\eta\pi^0$) with a missing (undetected) photon, and from genuine 5γ events (feedthrough

[9] We refrain from applying a kinematic fit to $\overline{p}p \to \pi^0\eta\gamma$ or $\overline{p}p \to \eta\eta\gamma$ since we want to study the $\omega \to 3\gamma$ Dalitz plot.

from $\pi^0\omega$ into $\eta\omega$ and $\eta\omega$ into $\pi^0\omega$ with $\omega \to \pi^0\gamma$).

Let us first deal with the 3-pseudoscalar final states. The Monte Carlo software generates $3\pi^0$, $2\pi^0\eta$ and $2\eta\pi^0$ events according to phase space. These events are submitted to the detector simulation based on GEANT3 and those with an undetected γ are submitted to the reconstruction procedure described above for $\pi^0\omega$ and $\eta\omega$ data events.

However, the Dalitz plots of 3-pseudoscalar final states, studied earlier by this Collaboration [13], show a rich resonance pattern and hence phase space distributed Monte Carlo events do not provide a faithful description of the background. The 3-pseudoscalar Monte Carlo events are therefore weighted according to their observed dynamics: The generated phase space distributed Dalitz plots are divided into cells of the same size as the measured 3-pseudoscalar Dalitz plots [13] and the weight of each Monte Carlo event is determined by the number of entries in the corresponding bin of the data Dalitz plots. To directly compare the Dalitz plots (fig. 2 and 3) with Monte Carlo generated plots, we normalize the Monte Carlo data sample to the number of $\overline{p}p$ annihilations in the all-neutral data sample. For instance for $2\pi^0\eta$, the weight of a Monte Carlo event falling into cell i is given by

$$W_i = \frac{N_0 f_i B(\overline{p}p \to 2\pi^0\eta) B(\eta \to 2\gamma) B(\pi^0 \to 2\gamma)^2}{N_i}. \tag{3}$$

N_0 is the number of annihilations (3.96×10^8), N_i the number of Monte-Carlo events in cell i and f_i the fraction of events in cell i of the real $2\pi^0\eta$ Dalitz plot. The $3\pi^0$ and $2\eta\pi^0$ events are treated similarly. The branching ratios B for $\overline{p}p$ annihilation into 3 pseudoscalars are taken from ref. [13]: $(6.2 \pm 1.0) \times 10^{-3}$ for $3\pi^0$, $(6.7 \pm 1.2) \times 10^{-3}$ for $2\pi^0\eta$ and $(2.0 \pm 0.4) \times 10^{-3}$ for $2\eta\pi^0$.

The background contributions to fig. 2 and 3 are listed in table 1. The $3\pi^0$ channel mainly contributes background under the π^0 bands in the $\omega \to 3\gamma$ Dalitz plots with negligible contributions under the η bands. The $2\pi^0\eta$ channel contributes about 300 events under the η bands in the $\pi^0\omega$ channel (fig. 2). This contribution, mainly from $a_2^0(1320)\pi^0$, dominates the background contribution to $\omega \to \eta\gamma$ in the $\pi^0\omega$ channel. Feedthrough from $2\eta\pi^0$ is negligible in the $\pi^0\omega$ channel but dominates the background contribution to the $\eta\omega$ channel with about 200 events under the η bands (fig. 3).

Next, we deal with the background from 5γ events. The channel $\pi^0\omega(\omega \to \pi^0\gamma)$ may contribute background to $\eta\omega(\omega \to 3\gamma)$ and the channel $\eta\omega(\omega \to \pi^0\gamma)$ background to $\pi^0\omega(\omega \to 3\gamma)$ due to combinatorial ambiguities in assigning the γ pairs to π^0 or η. In the simulation of $\pi^0\omega$ and $\eta\omega$ the angular distribution of the γ from $\omega \to \pi^0\gamma$ or $\eta\gamma$ must be taken correctly into account. The observed angular distribution for real $\pi^0\omega(\omega \to \pi^0\gamma)$ events has been fitted with a function of the form[10]

$$\frac{dN}{d\cos\theta} \propto 1 + b\cos^2\theta, \tag{4}$$

where θ is the angle of the γ in the ω rest frame and $b = 0.82 \pm 0.06$[11]. This angular distribution is then used to weight $\pi^0\pi^0\gamma$ and $\pi^0\eta\gamma$ Monte Carlo events. The ω peak is simulated by a Breit-Wigner amplitude. For the branching ratios we use $B(\overline{p}p \to \pi^0\omega) = (5.73 \pm 0.47) \times 10^{-3}$, $B(\overline{p}p \to \eta\omega) = (1.51 \pm 0.12)$ % [7] and $B(\eta \to 2\gamma) = (39.3 \pm 0.3)$ %, $B(\omega \to \pi^0\gamma) = (8.5 \pm 0.5)$

[10] Annihilation from $^3S_1$ atomic orbitals which dominates in liquid hydrogen leads to $b = 1$ while from $^1P_1$ one expects $b = 0$ or $b = -3/5$ depending on the relative angular momentum between π^0 and ω ($L = 0$ or 2).

[11] The measured γ angular distribution for $\eta\omega(\omega \to \pi^0\gamma)$ is similar ($b = 0.90 \pm 0.05$) [14].

% [15]. Applying the same normalization procedure as for 3-pseudoscalar events we find 130 background events mainly distributed under the η bands of fig. 2 and 76 background events mainly under the π^0 bands of fig. 3 (table 1).

5 $\omega \to \eta\gamma$ from the $\eta\omega$ channel

The branching ratio for $\omega \to \eta\gamma$ will be derived by normalizing on the known branching ratio for $\omega \to \pi^0\gamma$ [15]. Hence we first count the number of $\omega \to \pi^0\gamma$ events in fig. 3. We obtain $N_{\omega\to\pi^0\gamma} = 50,430 \pm 239$ events. The reconstruction efficiency, $\varepsilon_{\omega\to\pi^0\gamma} = (21.3 \pm 0.2)$ %, is obtained by Monte Carlo simulation.

We then select the $\omega \to \eta\gamma$ events in the Dalitz plot by rejecting events with at least one γ in the π^0 bands ($|E_\gamma - 379$ MeV$| < 10$ MeV). However, a π^0 peak is observed when plotting the 2γ-invariant mass with one γ from $\omega \to 3\gamma$ and the other from the recoiling η. These events are mainly due to $\eta\omega(\omega \to \pi^0\gamma)$ events for which the kinematic fit assigned wrong η and ω combinations. These events (with $|m_{\gamma\gamma} - 135$ MeV$| < 25$ MeV) are therefore removed. This cut also reduces the simulated background events in table 1 to a negligible amount except for the channel $2\eta\pi^0$.

The 3γ Dalitz plot has a sixfold symmetry. We therefore analyze only one sextant by plotting the γ energy distribution of the γ with the lowest energy in the ω rest frame. Figure 4 shows the γ energy distribution of real events and the simulated background distribution from $2\eta\pi^0$. Integrating the three bins around 200 MeV and subtracting the background we find $N_{\omega\to\eta\gamma} = 123 \pm 19$ $\omega \to \eta\gamma$ events. Figure 5 shows the background subtracted γ energy distribution. The shaded histogram shows the fit from the coupled channel analysis described in section 7. The slight excess of events below 150 MeV (see also fig. 4) may indicate a small systematic error in the background normalization (in particular in the assumed branching ratio for $\overline{p}p \to$ 0-prong) which is taken into account as systematic error in the number of signal events.

The reconstruction efficiency for $\eta\omega(\omega \to \eta\gamma)$ is calculated by Monte Carlo simulation: $\varepsilon_{\omega\to\eta\gamma} = (17.0 \pm 0.3)$ %. The ratio of branching ratios is then

$$\frac{B(\omega \to \eta\gamma)}{B(\omega \to \pi^0\gamma)} = \frac{N_{\omega\to\eta\gamma}}{N_{\omega\to\pi^0\gamma}} \cdot \frac{\varepsilon_{\omega\to\pi^0\gamma}}{\varepsilon_{\omega\to\eta\gamma}} \cdot \frac{B(\pi^0 \to 2\gamma)}{B(\eta \to 2\gamma)} = (7.69 \pm 1.19) \times 10^{-3}, \tag{5}$$

or, using the known branching ratio $B(\omega \to \pi^0\gamma) = (8.5 \pm 0.5)\%$ [15],

$$B(\omega \to \eta\gamma) = (6.5 \pm 1.1) \times 10^{-4}. \tag{6}$$

The error is dominated by the error on the number of observed $\omega \to \eta\gamma$ events. The systematic errors on the reconstruction efficiencies cancel in good approximation. Our branching ratio (6) is in good agreement with the result from ref. [6] $(8.3 \pm 2.1) \times 10^{-4}$ which was measured by suppressing ρ production.

The $2\eta\gamma$ final state is also investigated by an alternative method. Rather than identifying the $\omega \to 3\gamma$ first and then measuring the energy peak of the photon recoiling against the η, the η or π^0 from ω decay is identified first. The $\eta\gamma$ and $\pi^0\gamma$ invariant mass distributions show peaks at the ω mass. In the absence of background, this and the previous approaches are equivalent.

Background from 3-pseudoscalar final states ($2\pi^0\eta$ and $2\eta\pi^0$) with a missing γ is suppressed by processing the data first with a lower γ- energy threshold of 4 MeV, in order to efficiently tag soft γ's from one of the π^0's that might be ignored otherwise. Events that form $2\pi^0$ or $\pi^0\eta$ with or without additional photons are removed. In a second step the surviving events are reprocessed with the higher γ energy threshold of 20 MeV and requiring exactly 5γ to suppress split-offs.

A $\chi^2 < 3$ test to 2γ-invariant masses compatible with the η mass is applied to select η's. Misidentified pions from the $\omega \to \pi^0\gamma$ channel can leak through to the $2\eta\gamma$ channel. Thus, pions are identified by requiring 2γ-invariant masses in a rather wide window of 85 to 185 MeV, based on Monte Carlo observations of the long tails in the measured $\pi^0 \to 2\gamma$ invariant mass distribution.

The $2\eta\gamma$ and $\pi^0\eta\gamma$ Dalitz plots show the rare decay $\omega \to \eta\gamma$ and the reference decay $\omega \to \pi^0\gamma$, respectively. They, however, still contain residual background from $\bar{p}p \to 6\gamma$. They are therefore fitted simultaneously (but incoherently) with events from five Monte Carlo simulated channels, namely $2\eta\pi^0$, $2\pi^0\eta$, $\eta(\omega \to \pi^0\gamma)$, $\eta(\omega \to \eta\gamma)$ and $\eta(\rho^0 \to \eta\gamma)$. The fit finds 1000 ± 70 $2\eta\pi^0$ events, 168 ± 18 $\eta(\omega \to \eta\gamma)$ signal events and 31 ± 12 $\eta(\rho^0 \to \eta\gamma)$ events in the $2\eta\gamma$ Dalitz plot. In the $\pi^0\eta\gamma$ Dalitz plot the fit finds 62,400 $\pm$ 400 $\eta(\omega \to \pi^0\gamma)$ signal events and $30,000 \pm 2000$ $2\pi^0\eta$ events. These numbers agree very well with expectations based on previously tabulated branching ratios and the absolute number of annihilations. Systematic errors were estimated by varying the cuts on the π^0 and η identification and observing systematic differences between Monte Carlo simulation and data. After correcting for Monte Carlo efficiencies one obtains the ratio of branching ratios

$$\frac{B(\omega \to \eta\gamma)}{B(\omega \to \pi^0\gamma)} = (8.0 \pm 0.9_{stat} \pm 1.3_{sys}) \times 10^{-3}, \tag{7}$$

leading to the result

$$B(\omega \to \eta\gamma) = (6.8 \pm 1.4) \times 10^{-4}, \tag{8}$$

which corroborates the analysis described above (eqn. 6). Including the coherent term in the summation of $\rho^0 \to \eta\gamma$ and $\omega \to \eta\gamma$ amplitudes changes the result slightly, by -10% for constructive interference and by +20% for destructive interference. A detailed account of this alternative analysis is given in ref. [14].

6 $\omega \to \eta\gamma$ from the $\pi^0\omega$ channel

For normalization purposes we again count the number of $\omega \to \pi^0\gamma$ events in fig. 2. We obtain $N_{\omega\to\pi^0\gamma} = 55,340 \pm 363$ events. The reconstruction efficiency, $\varepsilon_{\omega\to\pi^0\gamma} = (23.9 \pm 0.2)$ %, is obtained by Monte Carlo simulation.

The $\omega \to \eta\gamma$ events are then selected following the procedure described in the previous section. We first remove events with at least one γ in the π^0 bands ($|E_\gamma - 379$ MeV$| < 15$ MeV). We select a somewhat larger π^0 cut than in the previous section to reduce background contribution from $2\pi^0\eta$ which often generates a γ near the π^0 bands.

As pointed out earlier, the main background arises from the channel $\overline{p}p \to \pi^0 a_2^0(1320)$, $a_2^0 \to \pi^0\eta$: Consider the reaction $\overline{p}p \to \pi_A^0 a_2^0$, $a_2^0 \to \pi_B^0\eta$. If one photon γ_1 from π_A^0 is not detected while the second photon γ_2, together with the $\eta \to \gamma_3\gamma_4$, fall in the ω mass region ($\omega \to \gamma_2\gamma_3\gamma_4$),

then the event fakes a perfect $\pi^0\omega(\omega \to \eta\gamma)$ event. The single γ of the faked $\pi^0\omega$ event lies dominantly in the region where its momentum is parallel to the ω-momentum. A cut is therefore applied to remove those events that fake an $\omega \to \eta\gamma$ signal, rejecting events for which the angle of the γ with respect to the ω direction is smaller than 45° for anyone of the 3 γ's. The residual background events are given in parentheses in table 1.

The background subtracted γ-energy distribution is shown in fig. 6 together with the fit from section 7. Integrating the four bins around 200 MeV we find $N_{\omega\to\eta\gamma} = 147 \pm 25$.

The $\omega \to \eta\gamma$ reconstruction efficiency is estimated by Monte Carlo simulation with weighted $\pi^0\eta\gamma$ events to simulate the Breit-Wigner and the $\omega \to \eta\gamma$ angular distribution: $\varepsilon_{\omega\to\eta\gamma} = (10.4 \pm 0.2)$ %. We then obtain the ratio of branching ratios

$$\frac{B(\omega \to \eta\gamma)}{B(\omega \to \pi^0\gamma)} = \frac{N_{\omega\to\eta\gamma}}{N_{\omega\to\pi^0\gamma}} \cdot \frac{\varepsilon_{\omega\to\pi^0\gamma}}{\varepsilon_{\omega\to\eta\gamma}} \cdot \frac{B(\pi^0 \to 2\gamma)}{B(\eta \to 2\gamma)} = (15.4 \pm 2.7) \times 10^{-3}, \tag{9}$$

leading to

$$B(\omega \to \eta\gamma) = (13.1 \pm 2.4) \times 10^{-4}, \tag{10}$$

larger than our previous result eqn. (6). We shall argue below that the discrepancy arises from coherent ρ production in $\overline{p}p \to \eta\rho^0$ and $\pi^0\rho^0$.

7 $\rho - \omega$ mixing

7.1 Formalism

The strength of the $\omega \to \eta\gamma$ signal is influenced by the channels $\overline{p}p \to \eta\rho^0$ and $\pi^0\rho^0$ which interfere with $\eta\omega$ and $\pi^0\omega$ through $\rho - \omega$ mixing. Using the branching ratios for $\omega \to \eta\gamma$ and $\rho^0 \to \eta\gamma$ from ref. [4] and [6] one predicts with the known two-body branching ratios [7, 8]

$$\frac{B(\overline{p}p \to \eta\omega)}{B(\overline{p}p \to \eta\rho^0)} \cdot \frac{B(\omega \to \eta\gamma)}{B(\rho^0 \to \eta\gamma)} \simeq 6 >> \frac{B(\overline{p}p \to \pi^0\omega)}{B(\overline{p}p \to \pi^0\rho^0)} \cdot \frac{B(\omega \to \eta\gamma)}{B(\rho^0 \to \eta\gamma)} \simeq 0.7 \tag{11}$$

One therefore expects a much stronger effect from $\rho - \omega$ mixing in $\pi^0\omega$.

Consider the isospin breaking electromagnetic $\rho - \omega$ transition. The mass matrix is given by [16]

$$M = \begin{pmatrix} m_\rho - i\Gamma_\rho/2 & -\delta \\ -\delta & m_\omega - i\Gamma_\omega/2 \end{pmatrix}. \tag{12}$$

Coleman and Glashow [17] have related the matrix element δ to the SU(3) breaking mass splitting of mesons and baryons, predicting $\delta \approx 2.5$ MeV, in good agreement with the experimental result, (2.48 ± 0.17) MeV, from $\omega, \rho \to \pi^+\pi^-$ [20]. The amplitude S for the reaction $\overline{p}p \to X(\rho - \omega) \to X\eta\gamma$ is, with m the $\eta\gamma$ invariant mass:

$$S = (A_\rho, A_\omega) \cdot (m - M)^{-1} \cdot \begin{pmatrix} T_\rho \\ T_\omega \end{pmatrix}, \tag{13}$$

or, up to an arbitrary phase factor,

$$S = \frac{|A_\rho||T_\rho|}{P_\rho}\left(1 - \frac{|A_\omega|}{|A_\rho|}\frac{e^{i\alpha}\delta}{P_\omega}\right) + e^{i\alpha}e^{i\phi}\frac{|A_\omega||T_\omega|}{P_\omega}\left(1 - \frac{|A_\rho|}{|A_\omega|}\frac{e^{-i\alpha}\delta}{P_\rho}\right), \tag{14}$$

in first order in δ. A is the production and T the decay amplitude of the two mesons and $P_\rho \equiv m - m_\rho + i\Gamma_\rho/2$, $P_\omega \equiv m - m_\omega + i\Gamma_\omega/2$. The relative phase between the production amplitudes A_ρ and A_ω is α while the relative phase between the decay amplitudes T_ρ and T_ω is ϕ. In the absence of $\rho - \omega$ interference ($\delta = 0$) eqn. (14) reduces to a sum of two Breit-Wigner functions with relative phase $\alpha + \phi$. The magnitudes of the amplitudes A and T are given by

$$\begin{aligned} |A_{\rho,\omega}| &= \sqrt{B(\overline{p}p \to X\rho,\omega)}\ , \\ |T_{\rho,\omega}| &= \sqrt{B(\rho,\omega \to Y)\Gamma_{\rho,\omega}}\ . \end{aligned} \tag{15}$$

where $\Gamma_{\rho,\omega}$ denotes the ρ or ω total width, Y their decay final state and $X = \pi^0$ or η.

For the $\pi^+\pi^-$ final state, the isospin violating decay amplitude $T(\omega \to \pi^+\pi^-)$ may be neglected leaving only the first term in eqn. (14). Hence one deals only with one relative phase α, the production phase, which depends on the production mechanism. This phase is predicted to be zero in e^+e^- and photoproduction and also in $\overline{p}p$ annihilation [18] but may be different from zero in other reactions. The $\rho - \omega$ interference has been observed by our collaboration in the channel $\overline{p}p \to \eta\pi^+\pi^-$ for which we found a phase α consistent with zero [19]. A value for α consistent with zero has also been measured in $\overline{p}p \to 2\omega, \rho\omega \to 2\pi^+2\pi^-\pi^0$ [20]. However, for the $\eta\gamma$ final state for which none of the decay amplitudes dominates, both α and ϕ contribute. The decay phase ϕ is either 0 or π (by time reversal arguments) but the quark model favours $\phi = 0$.

Our data are mostly sensitive to the relative phase $\alpha+\phi$ between the two terms in eqn. (14). Thus constructive interference means that $\phi+\alpha = 0$ or π. We shall assume $\alpha = 0$ in the analysis below (according to ref. [18, 19, 20]) and determine the decay phase ϕ.

The solution $\phi = \alpha = 0$ corresponds to the constructive interference solution in $\rho, \omega \to \eta\gamma$ in e^+e^- [4] while $\phi = \pi$, $\alpha = 0$ corresponds to their destructive interference solution. We shall show that our $\omega \to \eta\gamma$ branching ratio is consistent with their constructive interference solution.

7.2 Coupled analysis of $\pi^0\omega$ and $\eta\omega$

The intensity $|S|^2$ (eqn. (14)) is used to weight phase space distributed Monte Carlo events. We generate 105,000 $\pi^0\eta\gamma \to 5\gamma$ events (for $\pi^0\omega$) and 100,000 $\eta\eta\gamma \to 5\gamma$ events (for $\eta\omega$) which are reconstructed following the same procedure as real data, including all cuts. In addition, we multiply the weight by the γ angular distribution for $\omega \to \eta\gamma$, eqn. (4). The two Monte Carlo samples are normalized to the number of expected $\pi^0\omega$, respectively $\eta\omega$ events in the 0-prong data set.

For $\pi^0\omega$ and $\eta\omega$ we use the production branching ratios given above [7] and $B(\overline{p}p \to \pi^0\rho^0) = (1.72 \pm 0.27) \times 10^{-2}$ [21], $B(\overline{p}p \to \eta\rho^0) = (4.1 \pm 0.8) \times 10^{-3}$ [8]. The errors on the branching ratios are included in the error for the weight $|S|^2$.

The branching ratios for $\omega \to \eta\gamma$ and $\rho^0 \to \eta\gamma$ and the relative decay phase ϕ are now determined by comparing the number of Monte Carlo events $N^{MC}_{\eta\omega,\omega\to\eta\gamma}$ and $N^{MC}_{\pi^0\omega,\omega\to\eta\gamma}$ with the observed number of events, $N_{\eta\omega,\omega\to\eta\gamma} = 123 \pm 19$ and $N_{\pi^0\omega,\omega\to\eta\gamma} = 147 \pm 25$. The optimum set of parameters is found at the minimum of the function

$$d \equiv \frac{(N_{\pi^0\omega,\omega\to\eta\gamma} - N^{MC}_{\pi^0\omega,\omega\to\eta\gamma})^2}{\sigma^2_{\pi^0\omega,\omega\to\eta\gamma} + (\sigma^{MC}_{\pi^0\omega,\omega\to\eta\gamma})^2} + \frac{(N_{\eta\omega,\omega\to\eta\gamma} - N^{MC}_{\eta\omega,\omega\to\eta\gamma})^2}{\sigma^2_{\eta\omega,\omega\to\eta\gamma} + (\sigma^{MC}_{\eta\omega,\omega\to\eta\gamma})^2}. \tag{16}$$

The simulation method is time consuming and does not permit a continuous variation of the three parameters. Accordingly, we search within a 3-dimensional lattice . For the $\rho^0 \to \eta\gamma$ branching ratio we expect a value in the range between $(3.8 \pm 0.7) \times 10^{-4}$ for constructive interference and $(6.1 \pm 0.9) \times 10^{-4}$ for destructive interference [4, 5] and for $\omega \to \eta\gamma$ a value close to the result obtained above with the $\eta\omega$ channel.

We calculate the function d (eqn. (16)) on a 3-dimensional lattice (1331 points). The angle ϕ is varied beween $-50°$ and $+50°$. The $\omega \to \eta\gamma$ and $\rho^0 \to \eta\gamma$ branching ratios vary beween 0 and 2 B_ω and between 0 and 8 B_ρ, respectively. Here $B_\omega = B(\omega \to \eta\gamma) = 8.3 \times 10^{-4}$, suggested by ref. [6] and $B_\rho = B(\rho^0 \to \eta\gamma) = 3.8 \times 10^{-4}$ suggested by the constructive interference solution of ref. [4, 5]. The minimum is found at the lattice point $\phi = -20°$, $B(\omega \to \eta\gamma) = 0.8 B_\omega$ and $B(\rho^0 \to \eta\gamma) = 3.2 B_\rho$. Figure 7 shows a 2-dimensional contour plot of d as a function of $B(\omega \to \eta\gamma)$ and $B(\rho^0 \to \eta\gamma)$ and fig. 8 the behaviour of d as a function of ϕ around the optimum lattice point. We note that our $\pi^0\omega$ and $\eta\omega$ data are only selfconsistent for constructive $\rho - \omega$ interference (α =0, $\phi \sim 0$). This is illustrated in figs. 9 and 10.

To estimate the errors the measured numbers of events are varied within their errors and the coupled analysis is repeated. We obtain the final results:

$$\begin{aligned} B(\omega \to \eta\gamma) &= (6.6 \pm 1.7) \times 10^{-4}, \\ B(\rho^0 \to \eta\gamma) &= (12.2 \pm 10.6) \times 10^{-4}, \\ \phi &= (-20^{+70}_{-50})°. \end{aligned} \tag{17}$$

8 Discussion

The $\omega \to \eta\gamma$ branching ratio derived from the coupled analysis of the $\pi^0\omega$ and $\eta\omega$ channels is consistent with the one measured in the $\eta\omega$ channel, $(6.5 \pm 1.1) \times 10^{-4}$, assuming no $\rho - \omega$ mixing. The $\omega \to \eta\gamma$ branching ratio from $\pi^0\omega$ (eqn. (10)) is much larger due to strong constructive $\rho - \omega$ mixing.

A summary of all experimental results is given in table 2. Our $\omega \to \eta\gamma$ branching ratio is in good agreement with the less precise measurement, $(8.3 \pm 2.1) \times 10^{-4}$ [6] and with the less precise constructive interference solution in e^+e^- [4], $(7.3 \pm 2.9) \times 10^{-4}$. A reanalysis [22] of the latter data, including the triangle anomaly, leads to $(6.56^{+2.41}_{-2.55}) \times 10^{-4}$, in agreement with our value.

The decay phase ϕ measured here is consistent with zero[12]. The solution $\phi = (160^{+70}_{-50})°$ (and $\alpha = \pi$) also satisfies our data but is in contradiction (i) with theoretical predictions [18] (ii) with other data in $\overline{p}p$ annihilation [19, 20] and (iii) with the branching ratio for destructive interference in e^+e^-. Consistency between e^+e^- and our data implies constructive interference in e^+e^- and $\phi = 0$, in accord with the quark model. Our $\rho^0 \to \eta\gamma$ branching ratio is not competitive but agrees with previous measurements [4, 5].

The ratio $B(\omega \to \eta\gamma)/B(\omega \to \pi^0\gamma)$ can be predicted from SU(3):

$$\frac{B(\omega \to \eta\gamma)}{B(\omega \to \pi^0\gamma)} = \frac{1}{9} \frac{p_\eta^3}{p_{\pi^0}^3} \cos^2(54.7° + \theta) = 10.2 \times 10^{-3}, \tag{18}$$

[12] Conversely, fixing $\phi = 0$ and varying α leads to a value for α consistent with zero.

where p_π and p_η are the decay momenta in the ω rest frame and $\theta = -17.3^\circ$ [23] is the pseudoscalar mixing angle. We obtain from the present analysis

$$\frac{B(\omega \to \eta\gamma)}{B(\omega \to \pi^0\gamma)} = (7.8 \pm 2.1) \times 10^{-3}, \tag{19}$$

in agreement with SU(3). From SU(3) one also expects

$$\frac{\Gamma(\rho^0 \to \eta\gamma)}{\Gamma(\omega \to \eta\gamma)} = 9, \tag{20}$$

while we find, together with $\rho^0 \to \eta\gamma$ from ref. [4, 5], a ratio of 10.3 ± 3.3.

8.1 Search for the direct decay $\omega \to 3\gamma$

The direct decay $\omega \to 3\gamma$ is similar to the decay of $(^3S_1)$ orthopositronium into 3γ [24] and has not been observed so far. The energy distribution of the three photons in positronium decay can be found in ref. [25]. By analogy, the population in the $\omega \to 3\gamma$ Dalitz plot is expected to be almost homogeneous except for a slight increase close to its boundaries where the $\gamma's$ are collinear and one γ reaches its maximum energy (above $E_\gamma \sim 0.45 m_\omega$). We will therefore assume phase space distributed $\omega \to 3\gamma$ events. The edge region is of no concern here since we will derive an upper limit for the branching ratio using events in the center of the $\omega \to 3\gamma$ Dalitz plot.

We use the central region (defined by $234 < E_{\gamma_i} < 303$ MeV) of the $\pi^0\omega$ Dalitz plot (fig. 2) which contains only one event (6 entries) to obtain an upper limit for the $\omega \to 3\gamma$ branching ratio. With phase space distributed Monte Carlo events, the reconstruction probability in this region is $\varepsilon_{\omega\to 3\gamma} = (0.57 \pm 0.06)$ % including all cuts. The upper limit for the branching ratio (95% confidence level, corresponding to $N_{\omega\to 3\gamma} = 3$ events) is then

$$B(\omega \to 3\gamma) = \frac{N_{\omega\to 3\gamma}}{\varepsilon_{\omega\to 3\gamma}} \cdot \frac{\varepsilon_{\omega\to \pi^0\gamma}}{N_{\omega\to \pi^0\gamma}} \cdot B(\omega \to \pi^0\gamma) = 1.9 \times 10^{-4}. \tag{21}$$

This result improves on the previous upper limit reported by the GAMS collaboration in $\pi^- p \to 3\gamma n$ [26]: $B(\omega \to 3\gamma) < 2 \times 10^{-4}$ at 90% confidence level. Note that the upper limit eqn. (21) derived from the $\pi^0\omega$ channel includes the (unknown) contribution from $\rho \to 3\gamma$ through constructive $\rho - \omega$ interference.

9 Summary

Antiproton-proton annihilation at rest into $\pi^0\omega$ and $\eta\omega$ was used to analyze the $\omega \to 3\gamma$ Dalitz plot. We have derived an upper limit for the direct decay $\omega \to 3\gamma$ and have determined the branching ratio $B(\omega \to \eta\gamma)$ with two different methods, (i) directly from $\eta\omega$ for which $\rho - \omega$ interference is small and (ii) with a coupled analysis of $\pi^0\omega$ and $\eta\omega$. Our result improves on previous measurements and selects unambiguously the constructive $\rho - \omega$ interference solution.

10 Acknowledgement

We thank the technical staff of the LEAR machine group and of all the participating institutions for their invaluable contributions to the success of the experiment. We are grateful to Dr. W. Dunwoodie from SLAC for enlightening discussions. We acknowledge financial support from the German Bundesministerium für Bildung, Wissenschaft, Forschung und Technologie, the Schweizerischer Nationalfonds, the British Particle Physics and Astronomy Research Council, the US Department of Energy and the National Science Research Fund Committee of Hungary. N. Djaoshvili, F.-H. Heinsius and K.M. Crowe acknowledge support from the Alexander von Humboldt Foundation.

References

[1] P.J. O'Donnell, Rev. Mod. Phys. 53 (1981) 673

[2] R. Sekhar Chivukula and J.M. Flynn, Phys. Lett. 168B (1986) 127

[3] H.B. O'Connell, Phys. Lett. B354 (1995) 14

[4] S.I. Dolinsky et al., Z. Phys C42 (1989) 511

[5] D.E. Andrews et al., Phys. Rev. Lett. 38 (1977) 198

[6] D. Alde et al., Z. Phys. C61 (1994) 35

[7] C. Amsler et al. (Crystal Barrel Collaboration), Z. Phys. C 58 (1993) 175

[8] C. Amsler and F. Myhrer, Ann. Rev. Nucl. Part. Sci. 41 (1991) 219

[9] E. Aker et al. (Crystal Barrel Collaboration), Nucl. Instrum. Methods A321 (1992) 69

[10] C. Amsler et al. (Crystal Barrel Collaboration), Phys. Lett. B 311 (1993) 362

[11] C. Pietra, Diploma work, Universität Zürich, 1996

[12] R. Brun et al., Internal Report CERN DD/EE/84- 1, CERN 1987

[13] C. Amsler et al. (Crystal Barrel Collaboration), Phys. Lett. B 355 (1995) 425

[14] M. Lakata, PhD Thesis, Univ. of California, Berkeley (1996)

[15] Particle Data Group: Review of Particle Physics, Phys. Rev. D54 I (1996) 1

[16] A.S. Goldhaber, G.C. Fox and C. Quigg, Phys. Lett. 30B (1969) 249

[17] S. Coleman and S. Glashow, Phys. Rev. 134 (1964) B671

[18] N.N. Achasov and G.N. Shestakov, Sov. J. Part. Nucl. 9 (1978) 19

[19] A. Abele et al. (Crystal Barrel Collaboration), in preparation

[20] P. Weidenauer et al., Z. Phys. C59 (1993) 387

[21] B. Armenteros, B. French, High Energy Physics, (Academic, ed. E. H. S. Burhop), London, (1969) 237

[22] M. Benayoun, S.I. Eidelman and V.N. Ivanchenko, Z. Phys. C72 (1996) 221

[23] C. Amsler et al. (Crystal Barrel Collaboration), Phys. Lett. B 294 (1992) 451

[24] M. Deutsch, Progr. Nucl. Phys. 3 (1953) 131

[25] A. Ore and J. L. Powell, Phys. Rev. 75 (1949) 1696

[26] Yu. D. Prokoshkin and V. D. Samoilenko, Phys. Doklady 40 (1995) 273

Tables

Signal		62,853	54,865
	$N_{MC}(\times 10^3)$	$\pi^0\omega(\omega \to 3\gamma)$	$\eta\omega(\omega \to 3\gamma)$
$3\pi^0$	260	5,168 (0)	959 (0)
$2\pi^0\eta$	906	1,263 (311)	1,476 (8)
$2\eta\pi^0$	110	9 (5)	265 (161)
$\pi^0\eta\gamma$	105	130 (67)	76 (0)

Table 1: Summary of background events in the $\pi^0\omega$ and $\eta\omega$ data samples. The numbers in parentheses refer to the residual background after cutting the π^0 bands and applying the π^0 cut on $\eta\omega$ or the a_2 cut on $\pi^0\omega$ (see text). N_{MC} is the total number of generated Monte Carlo events.

Ref.	Reaction	$\omega \to \eta\gamma$ $[10^{-4}]$		$\rho^0 \to \eta\gamma$ $[10^{-4}]$		Relative phase $[^\circ]$
		$+$	$-$	$+$	$-$	
[5]	Photoproduction	$3.0^{+2.5}_{-1.8}$	29 ± 7	3.6 ± 0.9	5.4 ± 1.1	$\alpha = -11 \pm 38^a$
[4]	$e^+e^- \to \omega, \rho$	7.3 ± 2.9	35 ± 5	4.0 ± 1.1	7.3 ± 1.5	^{b}
[22]	$e^+e^- \to \omega, \rho$	$6.56^{+2.41}_{-2.55}$ ^{c}	–	$1.89^{+0.61}_{-0.78}$ ^{c}	–	^{b}
[6]	$\pi^-p \to \eta\gamma n$	8.3 ± 2.1^d		–		–
This work	$\overline{p}p \to \eta\omega$	6.6 ± 1.1^e		–		–
This work	$\overline{p}p \to \eta\omega, \pi^0\omega$	6.6 ± 1.7	–	12.2 ± 10.6	–	$\phi = -20^{+70}_{-50}$ ^{b}

Table 2: Experimental results for $\omega \to \eta\gamma$ and $\rho^0 \to \eta\gamma$. The symbols + and − refer to constructive ($\phi = 0$), respectively destructive interference ($\phi = \pi$).
[a] for the solution with constructive interference ($\phi = 0$)
[b] α fixed to 0
[c] reanalysis of data from ref. [4] including triangle anomaly
[d] suppressing ρ exchange
[e] neglecting $\rho - \omega$ interference

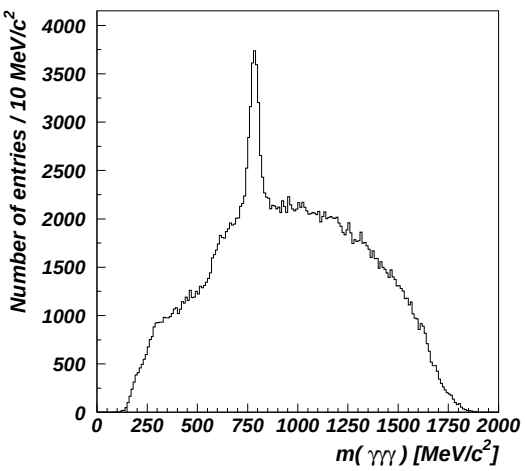

Figure 1: *3γ-invariant mass distribution for a subsample of the 5γ data.*

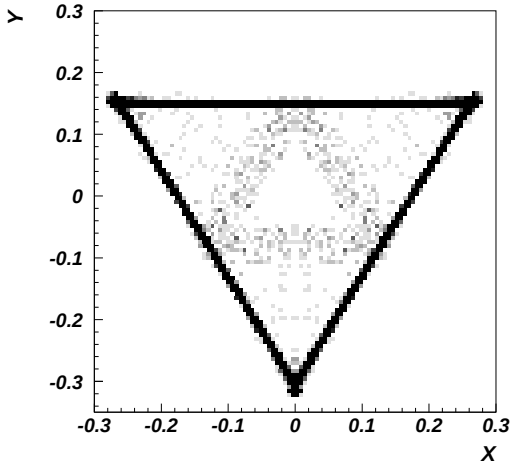

Figure 2: $\omega \to 3\gamma$ *Dalitz plot for* $\pi^0\omega$ *events (6 entries/event).*

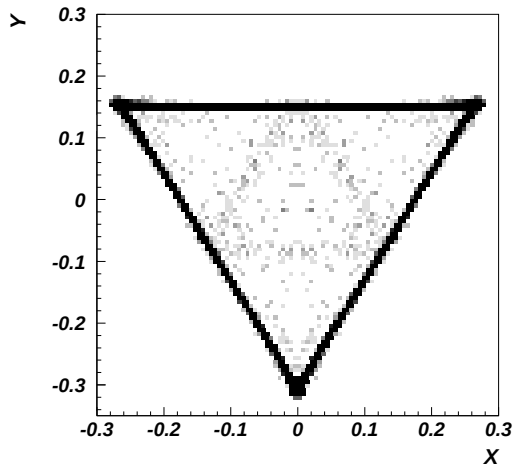

Figure 3: $\omega \to 3\gamma$ *Dalitz plot for* $\eta\omega$ *events (6 entries/event).*

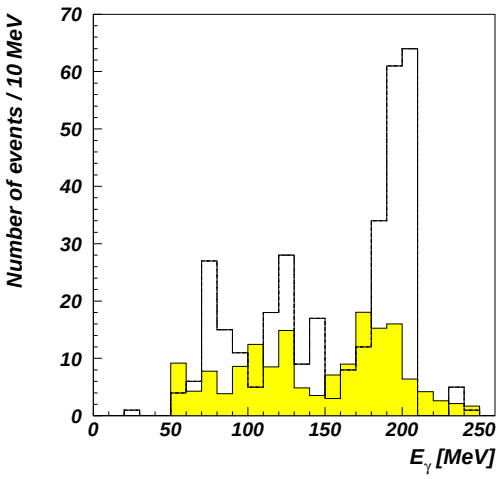

Figure 4: γ *energy distribution in the* ω *rest frame for* $\eta\omega(\omega \to 3\gamma)$ *events outside the* π^0 *band. Plotted is the* γ *with the lowest energy. The dark histogram shows the background contribution from* $2\eta\pi^0$.

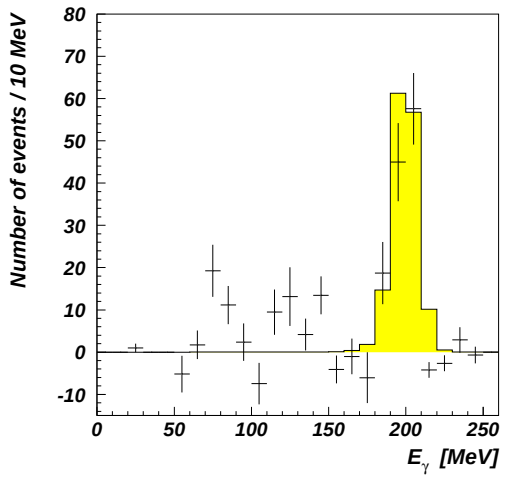

Figure 5: *Background subtracted* γ *energy distribution from* $\eta\omega$ *in the* ω *rest frame for events outside the* π^0 *bands. The dark histogram is the coupled channel fit described in the text.*

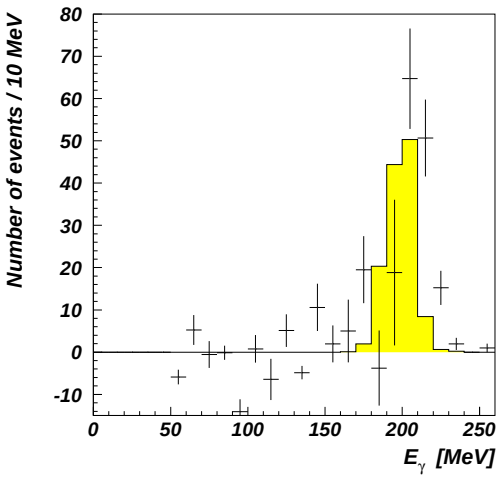

Figure 6: *Background subtracted* γ *energy distribution from* $\pi^0\omega$ *in the* ω *rest frame for events outside the* π^0 *bands. The dark histogram is the coupled channel fit described in the text.*

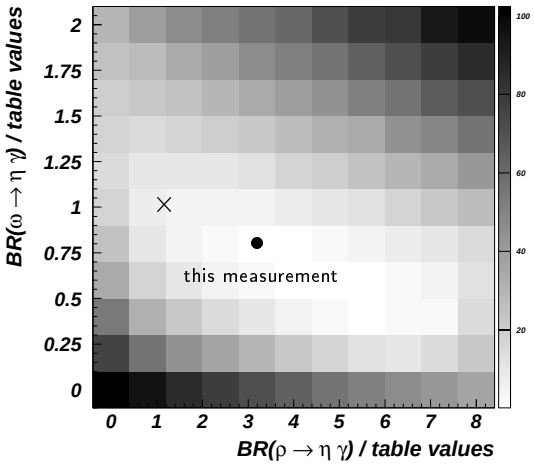

Figure 7: *Contour plot of the function d for* $\phi = -20°$. *The cross marks the point with branching ratios* B_ρ *and* B_ω.

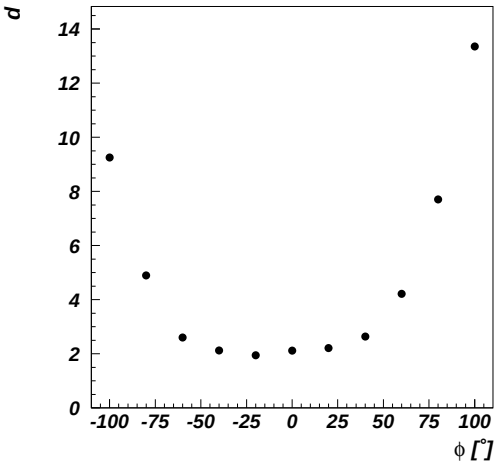

Figure 8: d *as a function of* ϕ *for* $B(\omega \to \eta\gamma) = 0.8B_\omega$ *and* $B(\rho^0 \to \eta\gamma) = 3.2B_\rho$. *The minimum value for* d *is at* $-20°$.

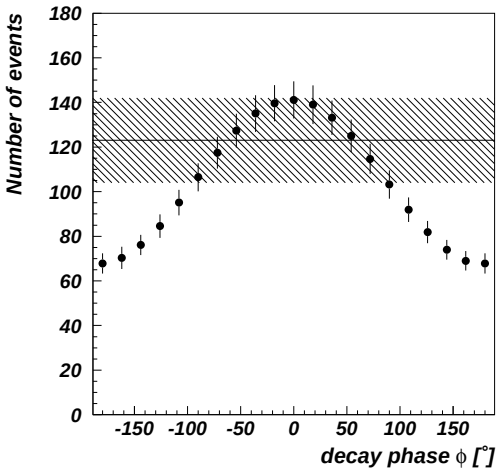

Figure 9: *Number of fitted* $\omega \to \eta\gamma$ *events in* $\eta\omega$ *as a function of the decay phase* ϕ. *The hatched region shows the* $(\pm 1\sigma)$ *range allowed by our* $\eta\omega$ *data.*

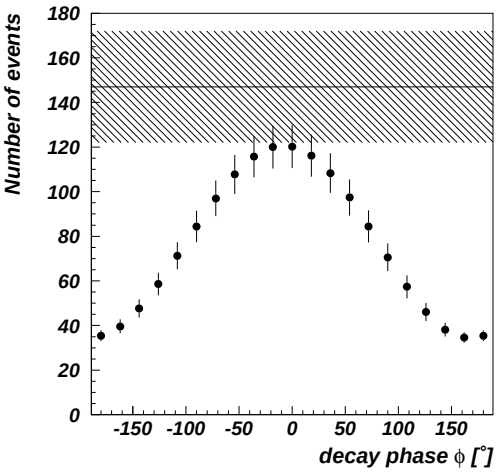

Figure 10: *Number of fitted* $\omega \to \eta\gamma$ *events in* $\pi^0\omega$ *as a function of the decay phase* ϕ. *The hatched region shows the* $(\pm 1\sigma)$ *range allowed by our* $\pi^0\omega$ *data.*